Similarities and Differences between the Subgenomic and Minus-Strand Promoters of an RNA Plant Virus

René C. L. Olsthoorn,†* P. C. Joost Haasnoot,‡ and John F. Bol

Institute of Biology, Gorlaeus Laboratories, Leiden University, 2300 RA Leiden, The Netherlands

Promoter regions required for minus-strand and subgenomic RNA synthesis have been mapped for several plus-strand RNA viruses. In general, the two types of promoters do not share structural features even though they are recognized by the same viral polymerase. The minus-strand promoter of *Alfalfa mosaic virus* (AMV), a plant virus of the family *Bromoviridae*, consists of a triloop hairpin (hpE) which is attached to a 3′ tRNA-like structure (TLS). In contrast, the AMV subgenomic promoter consists of a single triloop hairpin that bears no sequence homology with hpE. Here we show that hpE, when detached from its TLS, can function as a subgenomic promoter in vitro and can replace the authentic subgenomic promoter in the live virus. Thus, the AMV subgenomic and minus-strand promoters are basically the same, but the minus-strand promoter is linked to a 3′ TLS to force the polymerase to initiate at the very 3′end.

Plus-strand RNA viruses encode an RNA-dependent RNA polymerase (RdRp) that is used to multiply their genome, with or without the help of additional factors from the host. To initiate RNA synthesis on the right template and at the right position, the viral RdRp recognizes specific RNA elements in the plus and minus strands, so-called promoter sequences. Many plus-strand RNA viruses also produce one or more subgenomic (sg) mRNAs to express downstream open reading frames (ORFs). These sgRNAs are synthesized either from prematurely terminated minus strands or more commonly by internal initiation on the minus-strand template at a specific promoter sequence (reviewed in reference 12). The sg promoter (sgp) is usually located 3′ with respect to the transcription start site, analogous to RNA polymerase II-directed transcription of cellular genes. In contrast, the plus- and minus-strand promoters, in order to prevent loss of genetic information, are situated 5′ of their start site, similar to, for example, promoter sequences for transcription of tRNA genes by RNA polymerase III (reviewed in reference 21).

While the host cell makes use of different polymerases to transcribe its genes, most viruses have only one type of polymerase at their disposal, which has to recognize different types of promoters. Rather surprisingly, there exists little similarity in sequence or structure between these promoters within one viral genome (12). The question arises as to how a single type of RdRp recognizes promoters that are different in sequence and polarity. Here we have studied this problem for the *Alfalfa mosaic virus* (AMV).

AMV belongs to the family *Bromoviridae*, which consists of five genera of plant viruses with a tripartite positive-strand

RNA genome (reviewed in references 3 and 4). RNAs 1 and 2 of these viruses encode the viral subunits of the replicase. RNA3 is dicistronic and codes for a movement protein that is required for cell-to-cell movement and a coat protein (CP) that is needed for cell-to-cell and long-distance transport. CP is translated from a sg messenger, RNA4, which is coterminal with the 3′ 800 to 1,000 nucleotides (nt) of RNA3. Synthesis of sgRNA occurs by internal transcription on the minus strand of RNA3. The 3′ ends of the genomic RNAs of these viruses are tagged with a tRNA-like structure (TLS) that can be charged with tyrosine in the case of bromo- and cucumoviruses but not in the case of alfamo- and ilarviruses (reference 15 and references therein). TLSs are also found at the 3′ ends of the genomes of several other plant viruses (reviewed in reference 6). In addition to harboring the signals for the initiation of minus-strand synthesis, TLSs can accommodate other functions. The *Brome mosaic virus* (BMV) TLS has been shown to mediate assembly of BMV virions (5), whereas the TLS of *Turnip yellow mosaic virus* mediates the translation initiation of its polyprotein (2). The AMV TLS accommodates binding sites for the viral CP, which appears to have a regulatory function. CP binding was shown to favor the formation of a linear conformation at the expense of the TLS. In this linear conformation, minus-strand synthesis is inhibited while translation is stimulated (13).

Recently, we identified a triloop hairpin, hpE, in the 3′ untranslated region (UTR) of the genomic RNAs of AMV as the essential promoter element for minus-strand synthesis by the purified AMV RdRp (Fig. 1A). We noticed that this structure, despite its completely different sequence, shares some features with the hairpin required for sgRNA synthesis (Fig. 1B). Both hairpins have in common a 10-bp stem that is interrupted between the fourth and fifth base pair from the top by a 3′ bulge and a trinucleotide hairpin loop. Fundamentally different are their locations: the sgp hairpin is situated just five bases downstream (3′) of the initiation site, whereas hpE is located more than 100 bases upstream (5′) of the transcriptional start. Interestingly, removal of these 100 bases that constitute the 3′ TLS triggered transcription from a site located
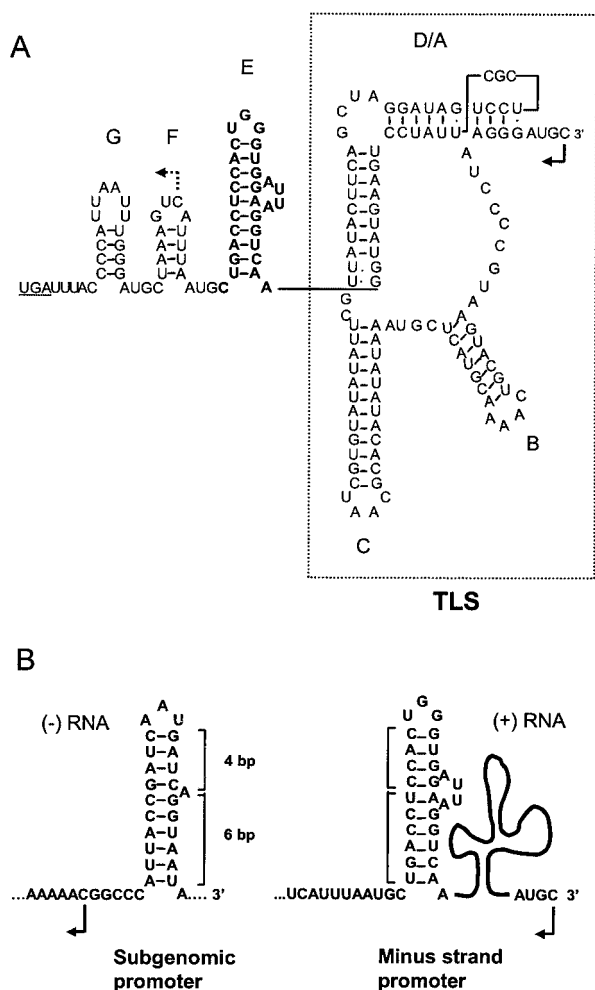
FIG. 1. (A) The 3′ UTR of AMV RNA3. hpE is shown in boldface type. The TLS is shown within the dotted box. The hooked arrow marks the transcriptional start site for minus-strand RNA synthesis; the dotted arrow indicates a cryptic initiation site that is activated upon deletion of the TLS. The TLS is depicted as a cloverleaf. (B) Secondary structure of the hairpins required for sg (left) and minus-strand (right) promoter activity.

FIG. 2. Constructs to assay minus-strand promoter activity of the sgp hairpin in vitro. (A) Left, E-TLS, template RNA corresponding to the 3′ terminal 140 nt of RNA3. Two G residues were added on the 5′ side for technical reasons. The product obtained with E-TLS is 142 nt. Right, sgp-TLS. The sgp hairpin is fused 5′ to the TLS of the 3′UTR of RNA3. The expected product with sgp-TLS is 139 nt. Center, autoradiogram of a gel showing ^{32}P-labeled products obtained after in vitro transcription with AMV RdRp. (B) Left, the structure of GF-sgp-TLS and a derivative (GF-sgp4-TLS) which has the bulge loop of hpE. Right, autoradiogram of a gel showing products obtained with the indicated templates. 3′ UTR, 3′ UTR of RNA3 (Fig. 1A); int., products originating from internal transcription at C-150; 3′, terminal transcription products.

upstream of hpE in vitro. On the basis of these observations, we proposed that hpE and the sgp hairpin are equivalent in binding the RdRp but that additional contacts with the TLS are needed to force the RdRp to transcribe from the very 3′ end of the genome (14). Here we show that hpE, when detached from the TLS, can function as an sgp in vitro and can effectively replace the authentic sgp in the live virus.

MATERIALS AND METHODS

Construction of RNA templates for in vitro RdRp assays. In vitro RdRp assays were carried out as described previously (14). RNA templates for these assays were generated by T7 RNA polymerase transcription of DNA fragments generated by PCR on plasmid 3kWT, which contains a full-length copy of AMV RNA3 or one of its derivatives, as described previously (14). sgp-TLS (Fig. 2) was generated by PCR with primers T7SP2 (5′-**AATTTAATACGACTCACTATA**G GATTACCGATCAATGATCAGGTAATAGGTATGAAGTCCTATTCG C-3′; the T7 promoter sequence is shown in boldface type) and WT2 (5′-G CATCCCTTAGGGGCATTCAT-3′). GF-sgp-TLS was obtained by a two-step PCR: first, two overlapping fragments were synthesized by using primer
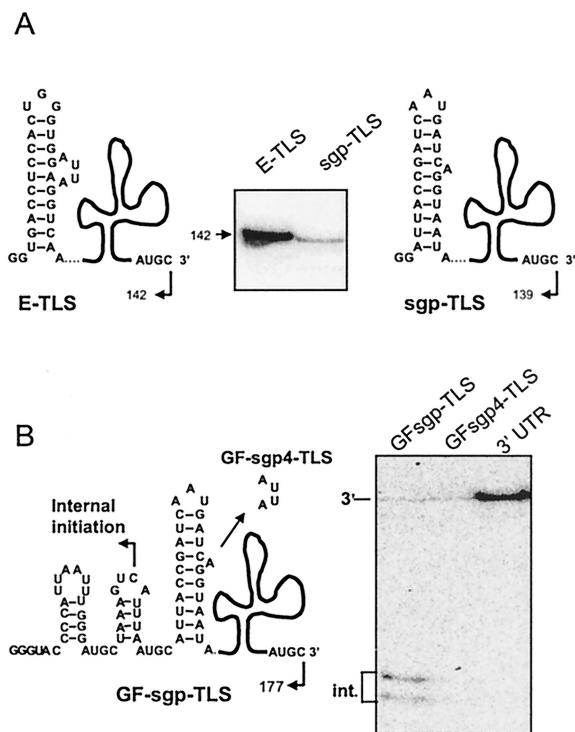
pairs T7G (5′-**AATTTAATACGACTCACTATA**GGGTACCCCATTAATTTG G-3′) and SPREV (5′-CCTGATCATTGATCGGTAATGCATTAAATGAC TTTAGCATCC-3′) and SP3 (5′-CATTACCGATCAATGATCAGGTAATA GGTATGAAGTCCTATTCGC-3′) and WT2 on plasmid 3kd5, a derivative of 3kWT lacking hpE (14). The overlapping PCR fragments were purified from gel and fused by a second PCR with T7G and WT2. GF-sgp4-TLS was also obtained by using this procedure, but the primer pairs were T7G and SPR (5′-CCTAATGATCATTGATCGGTAATGCATTAAATGACTTTAG CATCC-3′) and SP4 (5′-CATTACCGATCAATGATCATTAGGTAATAAG GTATGAAGTCCTATTCGC-3′) and WT2. The construction of GFE-TLS (or 3′ UTR) and E-TLS has been described previously (14). TLS-E (Fig. 3) was obtained in a single PCR with primers T7D (5′-**AATTTAATACGACTC ACTATA**GGGTATGAAGTCCTATTCG-3′; T7 promoter in boldface type) and 3′E (TTGACCTTAATCCACCCAGTGGAGGTCAGAATCGCATCCC TTAGG-GGCATTCATG-3′) on 3kWT. TLS-Ei was obtained with primers T7D and 3′EA (5′-TTGACCTTAATCCACCCAGTGGAGGTCAGAATCT CATCCCTTAGGGG-3′) on TLS-E. TLS-sgp was obtained with T7D and 3′SP (5′-GATGAAATATTACCTGATCATTGATCGGTAATGAATCGCA TCCCTTAGGGGCATTCATG-3′) on 3kWT. TLS-Bsp was obtained with primers T7D and 3′BSP (5′AAAAAAAGATCTATGTCCTAATTCAGCGT ATCCCTTAGGGGCATTCATG-3′) on 3kWT. sgp (Fig. 4) was obtained by PCR on 3kWT with primers −37 (5′-GATGAAATATTACCTGATCG-3′) and T7154 (5′-**AATTTAATACGACTCACTATA**GGGGACTTTCAACGCCGG AGG-3′). sgpE was obtained with primers SGPE (5′-GCATCTCTTATTGA CCTTAATCCACCCAGTGGAGGTCAGGGGCCGTTTTTATTTTTAATTT TC-3′) and T7154. sgpE37 was obtained with primers SGPE2 (5′-GATGAA

FIG. 3. Constructs to assay sgp activity of hpE in vitro. (A) E-TLS (Fig. 2). The spacing between hpE and TLS in TLS-E RNA was chosen to resemble the spacer in the wild-type sgp (Fig. 1B). The expected size of sgRNA directed by TLS-E is 113 nt. The autoradiogram shows products obtained above each lane. TLS, template corresponding to 3′-terminal 113 nt of RNA3. The sgp from minus-strand RNA3 yields a fragment of 154 nt. Template activities are indicated as a percentage of the 3′ UTR template activity and are corrected for the number of incorporated ^{32}P-UMP residues. (B) In TLS-Ei, the transcription initiation site was inactivated by mutation to an A residue. In TLS-sgp, the TLS is fused to nt −5 to −37 of the AMV sgp region (8). In TLS-Bsp, the TLS is fused to nt −1 to −27 of the BMV sgp region (9).

FIG. 4. Effect on sgRNA synthesis of replacement of the sgp hairpin by hpE. sgp, promoter fragment corresponding to nt +154 to −37 of minus-strand RNA3 (transcriptional start site is taken as +1). For sgpE, nt −6 to −37 from sgp were replaced by the indicated sequence. Transcription from sgpE potentially yields products of 154 and 197 nt. For sgpEB1, the bulge loop of sgpE was reduced to a single nucleotide; putative products are 154 and 194 nt in length. For sgpE37, the sequences flanking the wild-type sgp hairpin were inserted 3′ of hpE in sgpE. The autoradiogram shows products obtained after in vitro transcription. Template activities are indicated as a percentage of the activity of the 3′ UTR template.

were obtained by cloning complementary oligonucleotides into DNA3 plasmids digested with EagI and NsiI. Synthesis of full-length RNA3 transcripts and inoculation of P12 tobacco plants were performed as described previously (15).

Northern blotting, RT-PCR, and sequencing. Total RNA was extracted from *Nicotiana tabacum* P12 leaves 5 days after inoculation, separated on a 1.5% agarose gel, and transferred to nylon membranes. Membranes were incubated with a ^{32}P-labeled RNA probe that is complementary to RNA3 and -4 as described previously (20). Total RNA was used for reverse transcription with avian myeloblastosis virus reverse transcriptase and an oligonucleotide (36-BIO) that is complementary to nt 1331 to 1355 of RNA3. The resulting cDNA was amplified by PCR using 36-BIO and oligonucleotide (P3FOR), which is homologous to nt 945 to 964 of RNA3. PCR products were sequenced (BaseClear, Leiden, The Netherlands).

ATTGACCTTAATCCACCCAG-3′) and T7154 on sgpE DNA. sgpEB1 was obtained with primers SGPE3 (5′-GCATCTCTTATTGACCTTCCACCCAG TG-3′) and T7154 on sgpE DNA.

Construction of an RNA3 vector for sgp analysis in vivo. Via PCR EagI and NsiI, restriction sites were introduced upstream and downstream of the hairpin, respectively, in a cDNA3 plasmid that contains a premature stop codon after the triplet encoding amino acid 255 of P3 (17). We also replaced the N-terminal amino acids of the CP ORF with those of a virulent strain that induces the formation of necrotic lesions on inoculated tobacco leaves (R. C. L. Olsthoorn, R. Miglino, and J. F. Bol, unpublished data). The desired promoter mutations

RESULTS

Can the sgp function as a minus-strand promoter? Because of the structural resemblances of the sgp hairpin and hpE (Fig. 1B), we wondered whether they could substitute for each other's functions. To investigate the potential minus-strand promoter activity of the sgp, the 24-nt fragment forming the sgp hairpin was fused upstream of the 3′-terminal 113 nt of RNA3. These 113 nt correspond to the TLS. In an in vitro assay using purified RdRp, this construct was capable of directing minus-strand RNA synthesis, albeit at only 18% of the level of the

control template E-TLS (Fig. 2A, lanes sgp-TLS and E-TLS). However, when preceded by upstream sequences of the 3′ UTR of RNA3—hairpins F and G—initiation from the 3′ terminus dropped to ~5% (Fig. 2B, compare lanes GFsgp-TLS and 3′UTR). At the same time, two shorter products appeared which probably originated from internal transcription at C-150 located in the loop of hpF. In a previous study, deletions in the TLS or decreases in the bulge size of hpE gave rise to the same two products, which were both shown to originate from transcription at C-150 (14). Attempts to increase 3′-terminal transcription with the GF-sgp-TLS construct by the introduction of the 4-nt bulge from hpE were not successful, although internal initiation was suppressed (Fig. 2B, lane GFsgp4-TLS). These results suggested that the sgp hairpin could not substitute for hpE in minus-strand promoter activity, presumably because it lacks the proper interactions with the TLS (see also Discussion).

Can hpE act as an sgp? We tested whether hpE can act as an sgp in two ways. First, hpE was moved from its original position 5′ to the TLS to a location 3′ of the TLS (Fig. 3A, lane TLS-E). In this context, hpE should be able to direct the synthesis of a minus-strand copy of the TLS. Indeed, TLS-E yielded a product of the expected size (113 nt) at an efficiency that equalled that of a template in which hpE was positioned 5′ to the TLS (lane E-TLS). Note that the TLS by itself is not active as a template at all (lane TLS). Mutation of the initiation site by changing it to an A residue abolished synthesis of the 113-nt product, implying that transcription started at the authentic C residue (Fig. 3B, lane TLS-Ei). Some oddly sized products were made on TLS-Ei, but they did not amount to more than 10% of the level obtained with TLS-E. Transcription from TLS-sgp, in which the authentic sgp was placed 3′ to the TLS, also yielded the 113-nt product at about the same level as did TLS-E (Fig. 3B, lane TLS-sgp). Introduction of the sgp from the distantly related BMV (9) resulted in small amounts of two products, of which one had the expected size (lane TLS-Bsp). Thus, the AMV RdRp does specifically recognize hpE and the sgp hairpin when they are taken out of their original context. Moreover, it is shown here that hpE can function as an sgp.

From the experiments just described, it seems that TLS-E and TLS-sgp are just as active as the wild-type 3′ UTR (GFE-TLS) or E-TLS. However, in competition experiments with the wild-type 3′ UTR, TLS-E and TLS-sgp were not good competitors, in contrast to E-TLS (data not shown). This finding showed that, although TLS-E has the same ingredients as E-TLS, it probably lacks the proper tertiary structure to be recognized efficiently by the RdRp.

In a second approach, the sgp present on a fragment of minus-strand RNA3 that is routinely used to measure activity of sgp hairpin mutants in vitro (8) was replaced by hpE plus 11 additional nucleotides. These 11 nt resemble the 3′ end of the plus-strand AMV RNAs and were added to investigate whether the RdRp would initiate transcription 3′ or 5′ of hpE. The wild-type sgp produced a 154-nt RNA, whereas hpE in this context gave rise to a product of the same size at a twofold-higher efficiency (Fig. 4, lanes sgp and sgpE). Template activity is indicated as a percentage of the level obtained with the wild-type 3′ UTR (lane 3′UTR). In addition, a faint product of approximately 200 nt was visible in lane sgpE that probably

originated from transcription 3′ of hpE at the terminal C residue. This 3′ end initiation was verified by mutant sgpEB1, which has a deletion of 3 nt in the bulge: the size of the 197-nt product became about 3 nt smaller as well (lane sgpEB1). This mutant also demonstrates that bulge size does not play a role in sgp activity, as it produces similar levels of sgRNA as does sgpE. Replacement of the 11 nt 3′ of hpE with those that are flanking the wild-type sgp decreased the sgRNA synthesis level to that of the wild-type sgp level (lane sgpE37). The influence of nucleotides at the 3′ side of this hairpin is presently unclear. These data once more show that hpE can function as an sgp in vitro.

Is hpE active as an sgp in vivo? To determine whether hpE is active as an sgp in vivo, we could not simply replace the sgp hairpin with hpE in the wild-type RNA3 clone, since this promoter is partly overlapping with the P3 ORF and amino acid changes in the C terminus of P3 were previously shown to be detrimental for RNA3 accumulation in plants. Therefore, we made use of an RNA3 mutant in which the P3 protein is lacking the C-terminal 54 amino acids by the introduction of a premature stop codon. This mutant was shown to accumulate to almost the wild-type level in locally infected leaves (17). By PCR mutagenesis, we engineered two restriction sites in the sgp region (Fig. 5A) and also replaced the N-terminal amino acids of the CP ORF with those of a virulent strain which induces the formation of necrotic lesions on inoculated tobacco leaves (R. C. L. Olsthoorn, R. Miglino, and J. F. Bol, unpublished data). The wild-type sgp hairpin was reintroduced into this RNA3 vector, yielding sWT, which was then inoculated onto P12 tobacco plants. P12 plants are transgenic and produce the AMV P1 and P2 replicase proteins. Inoculation with RNA3 results in the production of progeny RNA3 and its sg messenger RNA4 (18). Since the accumulation of RNA3 (and RNA4) is dependent on the expression of CP from RNA4, a defect in sgp activity, and thus RNA4 synthesis, will also affect the accumulation of RNA3. Plants inoculated with sWT showed lesions as soon as 36 h postinfection. Northern blot analysis of plus-strand RNAs isolated from the inoculated P12 leaves detected both RNA3 and -4, indicating that the introduced changes did not significantly affect viral replication (Fig. 5B, lane sWT).

Introduction of hpE in this RNA3 vector and subsequent inoculation of tobacco plants resulted in the formation of necrotic lesions and in the accumulation of RNA3 and -4 at levels comparable to that of sWT (Fig. 5B, lane sE). Sequencing of the viral RNA isolated from these plants revealed that the introduced changes were still present. This finding was also true for the constructs tested below. The sgp activity of sE was strongly dependent on base pairing in the upper part of the helix. Disruption of the upper C-G base pair (mutants sECC and sEGG) abolished accumulation of RNAs 3 and 4, whereas changing it to G-C restored RNA4 synthesis to almost wild-type levels (lanes sECC, sEGG, and sEGC). Similarly, breaking up all base pairs above the bulge interfered with sgp activity (lane sET1). However, restoring base pairing capacity by the compensatory changes did not restore promoter activity (lane sET2).

We note that in lane sEGC a strong band is present below RNA3 which could be a degradation product of RNA3 called RNA3′ (19). If true, this finding would suggest that the ratio
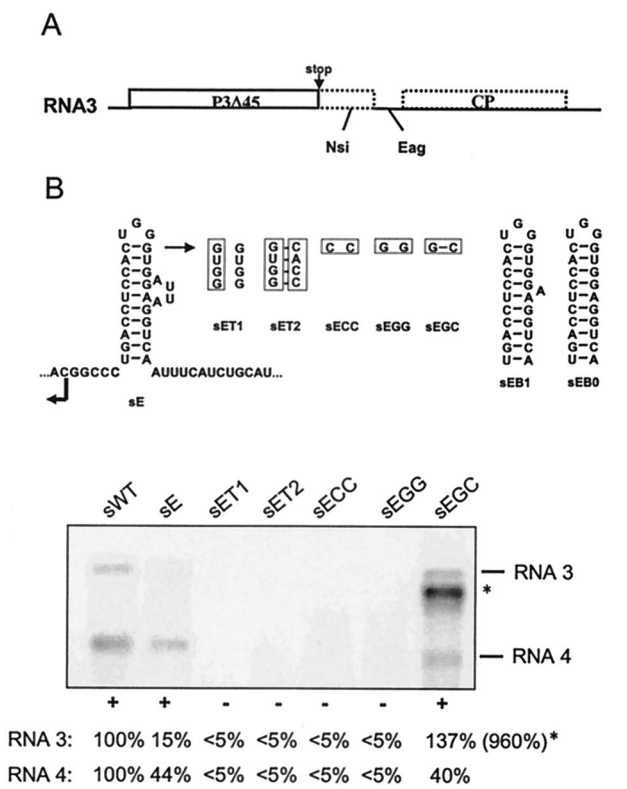
FIG. 5. In vivo system to test sgp activity of hpE. (A) RNA3 vector with truncated P3 protein and insertion of NsiI and EagI restriction sites. (B) RNA3 constructs in which the sgp hairpin has been replaced by hpE or mutants thereof. Northern blot shows RNA3 and -4 accumulation in P12 tobacco leaves. Results of two independent lesion assays are summarized below each lane. −, no necrotic lesions; +, >100 lesions developed per inoculated half-leaf over a period of 2 weeks. *, the position of a possible degradation product of RNA3 that is believed to lack the 5′-terminal 420 nt (19).

between RNA3 and -4 has been severely changed for this mutant. Alternatively, this band represents a dimer of RNA4 as a consequence of high levels of RNA4 in combination with incomplete denaturation of the RNA sample.

We expected that the size of the bulge loop would not have a significant effect on sgp activity (e.g., Figure 3A, lanes sgpE and sgpEB1), in accordance with previous results. Indeed, inoculation of plants with sEB1 or sEB0 RNA3 (Fig. 5B) led to similar levels of RNA3 and -4 accumulation and lesion numbers, as was true with sE (data not shown).

DISCUSSION

We have shown here that two apparently different types of promoters of the plus-strand RNA virus AMV share a common element: a 10-bp hairpin with a trinucleotide loop. These triloop hairpins, hpE and the sgp hairpin, likely constitute the main recognition site for the viral polymerase. In the absence of the TLS, hpE functioned as a bona fide sgp both in vitro and in vivo. The sgp hairpin, on the other hand, was only marginally functional as a minus-strand promoter when it was tied to the TLS. Also, the sgp hairpin was not functional in minus-strand RNA3 synthesis in vivo (R. C. L. Olsthoorn, unpublished

data). We attribute this low minus-strand promoter activity to a lack of tertiary interactions between this hairpin and the TLS. This result might be due in part to the size of the sgp hairpin's bulge (1 nt). We previously observed that by reducing hpE's bulge loop from 4 to 1 or 0 nt, transcription initiation from the 3′ end decreased, to the benefit of internal initiation from a site 5′ of this hairpin (14). Attempts to restore these putative contacts by introducing hpE's bulge loop in the sgp hairpin were only partially successful: internal initiation was decreased, but initiation from the 3′ end was not enhanced (Fig. 2B, lane GFsgp4-TLS). This finding can be interpreted in several ways, one being that the 4-nt bulge distorts the sgp hairpin in such a way that it can no longer be recognized by the RdRp. The small amount of 3′ end initiation that we still observe with GF-sgp-TLS and GF-sgp4-TLS must then be the result of aspecific recognition by the RdRp. Similar aspecific products have been described previously (14).

Apart from their length and the presence of a triloop, hpE and the sgp hairpin do not share many features, suggesting that any sequence that can fold into a 10-bp triloop hairpin will function as sgp. This supposition is basically true. We have found recently that the top 4 bp and the triloop nucleotides can be replaced by heterologous sequences and still yield infectious viruses as long as they form 4 bp and a (pseudo)triloop (10). Of course, depending on the nature of these 4 bp and loop nucleotides, not only the accumulation of RNA4 but also the ratio between RNA3 and -4 varied enormously. We observed something similar here when the C-G loop-closing base pair of hpE was mutated to G-C (sEGC). RNA4 accumulation remained comparable to that of sE, but RNA3 increased 9-fold (or even 63-fold if the extra band below RNA3 is indeed derived from RNA3). An alternative explanation could be that this band is an RNA4 dimer due to inefficient denaturation of the sample. The ratio between RNA3 and -4 (1:8) would then be similar to that of sE (1:9), but the total accumulation would be 10 times higher. Increased accumulation was also observed when the upper base pair of the sgp hairpin was changed to G-C in vivo (10) and in vitro (8). Remarkably, mirroring all 4 bp above the bulge loop in hpE completely eliminated RNA synthesis in vivo (Fig. 5, lane sET2). The same mutations in hpE in the context of the 3′ UTR were previously shown also to inhibit minus-strand RNA synthesis (14). It is therefore likely that the structure formed by these base pairs or their orientation with respect to the base pairs below the bulge is important for recognition as well. Future experiments will have to address the role of sequence specificity and structure.

In all in vitro assays done so far, it appears that the minus-strand promoter, e.g., 3′ UTR or E-TLS, is more active than the sgp (Fig. 4). This finding would imply that hpE is a better RdRp binder or promoter. However, when put in the same context as the sgp hairpin, its activity is the same as that of the wild-type sgp hairpin (Fig. 4, lane sgpE37). Conversely, sgp activity of the sgp hairpin can be enhanced severalfold by placing it 3′ to the TLS (compare Fig. 3B, lanes TLS-sgp and TLS-E, and Fig. 3A, lanes TLS-E and sgp). It should be noted that these effects could also result simply from changes of nucleotides flanking the initiation site, i.e., "...augCgauu..." in TLS-E might be more favorable for initiation than "...aaaaCggccc..." in sgpE. A fourfold increase in minus-strand synthesis in vitro was reported for changing the AAGC
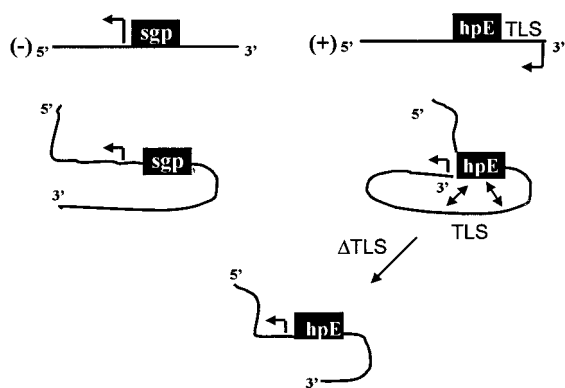
FIG. 6. Schematic representation of the role of the TLS in positioning the 3′ initiation site upstream of hpE (right), thereby resembling the sgp (left).

terminus to AUGC in a chimera consisting of RNA sequences from AMV and the ilarvirus *Prunus necrotic ringspot virus* (1).

Perhaps more difficult to understand is the effect of sequences 3′ of these hairpins (Fig. 4). sgpE was about twofold more active than sgpE37, which contained the wild-type sequence at its 3′ side. It is conceivable that the RdRp uses this 3′ sequence as a sort of step-up in binding to these hairpins and that the 3′ sequence of sgpE is better at this than that of sgpE37. This supposition could also explain why the longer product is formed only with sgpE and sgpEB1 (Fig. 4). Previously, maximal in vitro transcription was obtained with the sgp hairpin flanked by 8 nt or more at its 3′ side, although fragments longer than 8 nt had an enhancing effect in vivo (8). However, the identity of these 8 nt has not been the subject of investigation and so their role remains speculative.

In the absence of the TLS, the AMV RdRp shows a preference to start transcription 5′ of hpE. Even in the presence of a 3′ end resembling the terminal 11 nt of AMV RNAs, the RdRp has a 10-fold-higher preference for the 5′ side (Fig. 4, sgpE). To force the RdRp to transcribe from an initiation site 3′ of hpE can apparently be achieved by the presence of the TLS. How is this realized? A schematic representation of how the AMV RdRp could initiate either 5′ or 3′ of a promoter hairpin is illustrated in Fig. 6. Assuming that the RdRp, when bound to its promoter, has its catalytic center located 5′ of the promoter, putative interactions between hpE and the TLS are thought to fold back the very 3′ end into the active site of the RdRp. When these interactions are missing, by deletion of the TLS for example, an alternative initiation site 5′ of hpE might enter the catalytic center of the RdRp. This model thus illustrates how two types of promoters can be recognized by a single type of RdRp. Whether an hpE-like element also is involved in the synthesis of the genomic plus strands remains to be seen.

We previously showed that, in vitro, the BMV sgp hairpin and the hairpin required for minus-strand synthesis are functionally interchangeable to a certain extent (9). The sgp hairpin supported minus-strand synthesis at 10% of the wild-type level, while the minus-strand promoter hairpin stimulated sgp activity severalfold. It remains to be demonstrated whether the minus-strand promoter of BMV can function as an sgp in vivo.

Outside the family *Bromoviridae*, no (functional) homology between sg and minus-strand promoters has yet been found. Even sgp sequences from viruses with multiple sgps, such as *Barley yellow dwarf virus* (11) or *Tobacco mosaic virus* (7), do not share obvious homology. It will be of interest to see whether the triloop hairpin identified in the TLS of *Tobacco mosaic virus* (16) can replace one of the hairpins required for sgRNA synthesis (7).

REFERENCES

1. Aparicio, F., J. A. Sanchez-Navarro, R. C. L. Olsthoorn, V. Pallas, and J. F. Bol. 2001. Recognition of *cis*-acting sequences in RNA 3 of *Prunus necrotic ringspot* virus by the replicase of Alfalfa mosaic virus. J. Gen. Virol. 82:947–951.
2. Barends, S., H. H. Bink, S. H. van den Worm, C. W. A. Pleij, and B. Kraal. 2003. Entrapping ribosomes for viral translation: tRNA mimicry as a molecular Trojan horse. Cell 112:123–129.
3. Bol, J. F. 1999. Alfalfa mosaic virus and ilarviruses: involvement of coat protein in multiple steps of the replication cycle. J. Gen. Virol. 80:1089–1102.
4. Bol, J. F. 2003. Alfalfa mosaic virus: coat protein-dependent initiation of infection. Mol. Plant Pathol. 4:1–8.
5. Choi, Y. G., T. W. Dreher, and A. L. N. Rao. 2002. tRNA elements mediate the assembly of an icosahedral RNA virus. Proc. Natl. Acad. Sci. USA 99:655–660.
6. Dreher, T. W. 1999. Functions of the 3′-untranslated regions of positive strand RNA viral genomes. Annu. Rev. Phytopathol. 37:151–174.
7. Grdzelishvili, V. Z., S. N. Chapman, W. O. Dawson, and D. J. Lewandowski. 2000. Mapping of the tobacco mosaic virus movement protein and coat protein subgenomic RNA promoters in vivo. Virology 275:177–192.
8. Haasnoot, P. C. J., F. T. Brederode, R. C. L. Olsthoorn, and J. F. Bol. 2000. A conserved hairpin structure in *Alfamovirus* and *Bromovirus* subgenomic promoters is required for efficient RNA synthesis in vitro. RNA 6:708–716.
9. Haasnoot, P. C. J., R. C. L. Olsthoorn, and J. F. Bol. 2002. The brome mosaic virus subgenomic promoter hairpin is structurally similar to the iron-responsive element and functionally equivalent to the minus-strand core promoter stem-loop C. RNA 8:110–122.
10. Haasnoot, P. C. J., J. F. Bol, and R. C. L. Olsthoorn. 2003. A plant virus replication system to assay the formation of RNA pseudotriloop motifs in RNA-protein interactions. Proc. Natl. Acad. Sci. USA 100:12596–12600.
11. Koev, G., and W. A. Miller. 2000. A positive-strand RNA virus with three very different subgenomic RNA promoters. J. Virol. 74:5988–5996.
12. Miller, W. A., and G. Koev. 2000. Synthesis of subgenomic RNAs by positive-strand RNA viruses. Virology 273:1–8.
13. Neeleman, L., R. C. L. Olsthoorn, H. J. M. Linthorst, and J. F. Bol. 2001. Translation of a nonpolyadenylated viral RNA is enhanced by binding of viral coat protein or polyadenylation of the RNA. Proc. Natl. Acad. Sci. USA 98:14286–14291.
14. Olsthoorn, R. C. L., and J. F. Bol. 2002. Role of an essential triloop hairpin and flanking structures in the 3′ untranslated region of alfalfa mosaic virus RNA in in vitro transcription. J. Virol. 76:8747–8756.
15. Olsthoorn, R. C. L., S. Mertens, F. T. Brederode, and J. F. Bol. 1999. A conformational switch at the 3′ end of a plant virus RNA regulates viral replication. EMBO J. 18:4856–4864.
16. Osman, T. A., C. L. Hemenway, and K. W. Buck. 2000. Role of the 3′ tRNA-like structure in tobacco mosaic virus minus-strand RNA synthesis by the viral RNA-dependent RNA polymerase in vitro. J. Virol. 74:11671–11680.
17. Sanchez-Navarro, J. A., and J. F. Bol. 2001. Role of the alfalfa mosaic virus movement protein and coat protein in virus transport. Mol. Plant-Microbe Interact. 14:1051–1062.
18. Taschner, P. E. M., A. C. van der Kuyl, L. Neeleman, and J. F. Bol. 1991. Replication of an incomplete alfalfa mosaic virus genome in plants transformed with viral replicase genes. Virology 181:445–450.
19. van der Vossen, E. A. G., T. Notenboom, and J. F. Bol. 1995. Characterization of sequences controlling the synthesis of alfalfa mosaic virus subgenomic RNA in vivo. Virology 212:663–672.
20. Vlot, A. C., A. Menard, and J. F. Bol. 2002. Role of the alfalfa mosaic virus methyltransferase-like domain in negative-strand RNA synthesis. J. Virol. 76:11321–11328.
21. Willis, I. M. 1993. RNA polymerase III. Genes, factors and transcriptional specificity. Eur. J. Biochem. 212:1–11.